

Hot spots active-cooling micro-channel heat sink device, using electro-osmotic flow

Marwan F. Al-Rjoub¹, Ajit K. Roy², Sabyasachi Ganguli^{2,3}, Rupak K. Banerjee¹

¹Mechanical Engineering Department, University of Cincinnati, Cincinnati, OHIO, USA

²Thermal Sciences and Materials Branch (AFRL/RXBT), Air Force Research Laboratory, WPAFB, OHIO, USA

³University of Dayton Research Institute, Dayton, OHIO, USA

ABSTRACT

Non-uniform heat flux generated by microchips causes “hot spots” in very small areas on the microchip surface. These hot spots are generated by the logic blocks in the microchip bay; however, memory blocks generate lower heat flux in contrast. The goal of this research is to design, fabricate, and test an active cooling, micro-channel heat sink device that can operate under atmospheric pressure while achieving a high-heat dissipation rate with a reduced chip-backside volume, particularly for spot cooling applications. An experimental setup was assembled and electro-osmotic flow (EOF) was used thus eliminating the high pressure pumping system. A flow rate of 82 $\mu\text{L}/\text{min}$ was achieved at 400 V of applied EOF voltage. An increase in the cooling fluid (buffer) temperature of 9.6 °C, 29.9 °C, 54.3 °C, and 80.1 °C was achieved for 0.4 W, 1.2 W, 2.1 W, and 4 W of heating powers, respectively. The substrate temperature at the middle of the microchannel was below 80.5 °C for all input power values. Numerical calculations of temperatures and flow were conducted and the results were compared to experimental data. Nusselt number (Nu) for the 4 W case reached a maximum of 5.48 at the channel entrance and decreased to reach 4.56 for the rest of the channel. Nu number for EOF was about 10% higher when compared to the pressure-driven flow. It was found that using a shorter channel length and an EOF voltage in the range of 400 – 600 V allows application of a heat flux in the order of $10^4 \text{ W}/\text{m}^2$, applicable to spot cooling. For elevated voltages, the velocity due to EOF increased, leading to an increase in total heat transfer for a fixed duration of time; however, the joule heating was also elevated with increase in voltage.

Keywords: Electro-osmotic flow, Micro-scale heat exchanger, Hot spot cooling, zeta-potential

1 INTRODUCTION

Intensive computing devices are projected to generate heat flux values that can exceed $2.5 \times 10^6 \text{ W}/\text{m}^2$ [1]. With these high-heat generation rates, the conventional cooling techniques have been found to be inadequate. Instead of forcing air to flow over fins, liquid can be forced to flow through channels that are in contact with the devices' surface. Various methods are being used to drive a liquid

through micro-channels, which include pressure-driven techniques that use mechanical pumps or pressurized gases. Another approach is to use electro-osmotic flow pumping technique; this technique has no moving parts and needs less maintenance compared to mechanical pumps.

Jiang *et al* [2] designed a closed-loop, two-phase, micro-channel cooling system with an external EOF pump and a heat rejecter, where a maximum of 7 ml/min coolant flow rate was achieved, with a chip temperature maintained less than 120 °C. Laser *et al* [3] used the EOF through narrow deep micro-channels to reduce the temperature of the high-power density spots of microchips, 170 $\mu\text{L}/\text{min}$ of coolant flow was achieved at 400 V of applied EOF voltage. Zhang *et al* [4] tested a single micro-channel for the pressure distribution along the heating length and measured the temperature variations during the phase change, the flow was pressure-driven using a syringe pump. Jung *et al* [5] used a single micro-channel to study the heat transfer to nanofluids, and investigated the differences between nanofluids and pure water for convection heat transfer coefficient and friction factor. Eng *et al* [6] designed an electro-osmotic flow, silicon-based, heat spreader that generated a coolant flow rate of 0.2 $\mu\text{L}/\text{min}$ at 2 V/mm electric field; a 4 °C reduction in device temperature was achieved.

Dasgupta *et al* [7] of our group studied the effects of the applied-electric field and micro-channel wetted-perimeter on electro-osmotic velocity. These numerical and experimental studies found that, as the wetted perimeter increases, the electro-osmotic velocity decreases, and the electro-osmotic velocity increases as the applied electric field increases.

In this pilot study an integrated EOF pump of microchannel fluid flow systems was designed, fabricated, and tested. The device is a micro-scale heat exchanger with an integrated EOF pump designated for hot spot cooling applications. The initial design of the device consisted of an array of micro-channels that were connected by two reservoirs. These channels and reservoirs were etched on a silicon substrate. Various sequential processes were conducted on the substrate, which included cleaning, spin coating, soft baking, photolithography, development, hard baking, and etching. The substrate was then bonded to a polydimethyl siloxane (PDMS) cover. An experimental flow loop was designed that included a voltage power supply and a data acquisition system (DAQ) for

temperature measurement. As a validation for the experimental data, numerical calculations were also performed for a single channel. Numerical results were compared with the experimental data.

2 METHODS

2.1 Experimental Methods

The actively cooled micro-channel heat sink device was designed by introducing 20-parallel-micro-channels, where each channel had a 300 μm width, and 3 cm length. The channels depth was 100 μm . These channels were connected by two reservoirs at both ends. Fig. 1A shows a drawing of the actively cooled micro-channel heat sink device having multiple micro-channels and a single reservoir with dimensions.

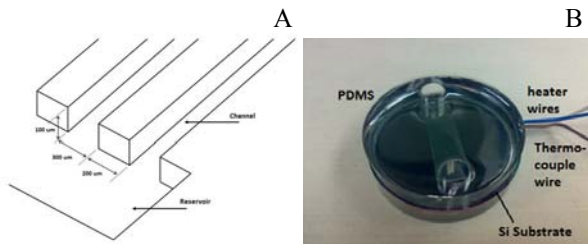


Fig. 1. A: Drawing of the actively cooled, micro-channel, heat sink device showing multiple micro-channels and a single reservoir; B: Photograph of the actively cooled micro-channel heat sink device.

A 2" $\langle 100 \rangle$ silicon substrate was selected. Channels and reservoirs were etched on it. Silicon etching was performed using KOH (potassium hydroxide) solution and the etching process was monitored to get the exact channel depth. At the end of the etching process a silicon dioxide layer was thermally grown on the channels surface. The silicon dioxide layer thickness was about 1 μm . This layer helped in creating a hydrophilic channel surfaces allowing EOF to occur. A similar heat spreader design by Eng *et al* [6] used a silicon dioxide layer with a thickness of 250 nm.

Instead of conventional fluid pumping techniques, EOF principle was implemented for which a power supply was required. A PDMS cover was introduced as a thermal insulator and to seal the top of the channels. A foil type DC powered heater was selected and attached to the bottom surface of the substrate. To vary the heat flux, a variable voltage DC power supply was used to power the heater. Voltages, currents, and temperatures were recorded using a DAQ system. A photograph of the actively cooled, micro-channel, heat sink device is shown in Fig. 1B. The wires, shown in Fig. 1B, were connected to a DC heater and to a thermocouple that was attached to the bottom surface of the silicon substrate. This thermocouple measured the substrate temperature at the middle of the microchannels.

The block diagram of the experimental flow loop is shown in Figure 2. The flow loop included the EOF

voltage power supply, a DC power supply, a DAQ system, thermocouples, and the actively cooled micro-channel heat sink device. The channel walls were treated with 1M NaOH (sodium hydroxide) solution in order to increase the surface charge. Then, the micro-channels within the heat sink device were filled with the cooling fluid (0.4 mM borax buffer, Ricca Chemical Company). The 0.4 mM borax buffer (cooling fluid) was used to conduct all the heat transfer experiments.

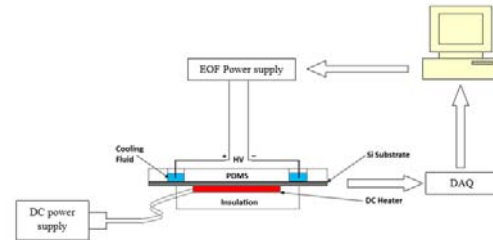


Fig. 2. Block diagram of the experimental flow loop

2.2 Numerical Methods

A 3D model of a single channel was constructed using CFD-GEOM (ESI-CFD Inc., Huntsville, AL). Structured meshing was used with 180,000 cells. The constructed channel had dimensions of 300 μm width, 3 cm length, and 100 μm depth which were equal to the physical channel dimensions. The boundary conditions used were zero pressures at the channel inlet and outlet, zero voltage at the outlet and EOF voltage value at the inlet ranging from 100 – 400 V. No slip condition was used for channel walls and the experimentally obtained zeta potential was used as a wall property. Constant wall heat flux was used as a wall boundary condition. Governing equations were solved using a multi-physics, finite volume solver. The algebraic multi-grid (AMG) solver was used to solve for the steady state coupled heat transfer, flow, and electric field through the channel. The convergence criterion was 10^{-6} .

2.3 Governing Equations

Electro-osmotic flow through the channel is governed by the continuity equation (1) and Navier–Stokes equation (2) [8].

$$\nabla \cdot u = 0 \quad (1)$$

$$\rho(u \cdot \nabla u) = \mu \cdot \nabla^2 u - \nabla p + f_e \quad (2)$$

where u is the cooling fluid (buffer) velocity (m/s), ρ is the cooling fluid (buffer) density (kg/m^3), μ is the dynamic viscosity of the cooling fluid (buffer) (Pa.s), p is the pressure inside the channel (Pa), and f_e is electro-osmotic force induced by the applied electric field ($f_e = \rho_e E$ where ρ_e is the bulk charge density, $\text{C} \cdot \text{m}^{-3}$ and E is the electric field, $\text{V} \cdot \text{m}^{-1}$). Equation (2) was written in terms of the applied electric potential, ϕ , (V) and the wall surface charge, ψ , ($\text{C} \cdot \text{m}^{-2}$) by Comandur *et al* [9] of our lab as shown in Equation (3).

$$\rho(u \cdot \nabla u) = \mu \nabla^2 u - \nabla p + \varepsilon \cdot (\nabla^2 \psi + \nabla \phi) \quad (3)$$

where ε is the cooling fluid (buffer) permittivity (C/V.m).

Steady state heat equation (4) was solved with a constant wall heat flux boundary condition at a constant inlet temperature of the cooling fluid. The solution was obtained for steady-state thermal distribution through the channel.

$$0 = \alpha_f \nabla^2 T - u \cdot \nabla T \quad (4)$$

where α_f is the cooling fluid (buffer) thermal diffusivity (m^2/s), T is the cooling fluid (buffer) temperature.

3 RESULTS

3.1 Cooling-fluid flow rate in microchannels

Cooling fluid flow rate through the micro-scale heat exchanger was $12.3 \mu\text{L}/\text{min}$ for each $2 \text{ V}/\text{mm}$ of applied electric field. The maximum flow rate achieved was $82 \mu\text{L}/\text{min}$ at 400 V of applied EOF voltage. Reynolds number (Re) was $0.1, 0.2, 0.3,$ and 0.4 for $100 \text{ V}, 200 \text{ V}, 300 \text{ V},$ and 400 V , respectively. It was found that the flow rate is proportional to the applied EOF voltage. As the electric field increases, the EOF velocity increases and thus, flow rate increases through the microchannels.

Velocity profiles for different values of applied EOF voltage are shown in Fig. 3. These profiles were generated using numerical calculations. It can be noticed that the velocities had a plug profile which is typically associated with the electro-osmotic flow. Such plug type velocity profile is expected to have higher heat transfer compared to parabolic flow profile as in the case of pressure-driven flow. The magnitude of the velocities ranged from $5.65 \times 10^{-4} \text{ m/s}$ at 100 V to $22.59 \times 10^{-4} \text{ m/s}$ at 400 V of applied EOF voltage.

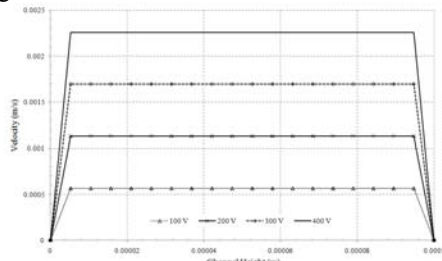


Fig. 3. EOF velocity profile for different applied EOF voltages

3.2 Heat transfer results for microchannels

The difference between the experimental channel outlet and inlet fluid temperatures at different heating power values for 400 V of applied EOF voltage are shown in Fig. 4. The 400 V of EOF voltage achieved the highest cooling fluid flow rate and hence had the best heat removal

performance. Heating power values were applied as follows: 0.4 W (heating power #1), 1.2 W (heating power #2), 2.1 W (heating power #3), and 4.0 W (heating power #4). The cooling fluid (buffer) temperature at the inlet reservoir was maintained at $23 \text{ }^\circ\text{C}$. For heating power #1 the measured outlet temperature difference ($T_{\text{channel outlet}} - T_{\text{channel inlet}}$) was $9.6 \text{ }^\circ\text{C}$, and the numerically calculated temperature difference at the outlet was $10.0 \text{ }^\circ\text{C}$. For heating power #2 the measured outlet temperature difference was $29.9 \text{ }^\circ\text{C}$, and the numerically calculated temperature difference at the outlet was $32.1 \text{ }^\circ\text{C}$. For heating power #3 the measured outlet temperature difference was $54.3 \text{ }^\circ\text{C}$, and the numerically calculated temperature difference at the outlet was $58.6 \text{ }^\circ\text{C}$. For heating power #4 the measured outlet temperature difference was $80.1 \text{ }^\circ\text{C}$, and the numerically calculated temperature difference at the outlet was $89.0 \text{ }^\circ\text{C}$.

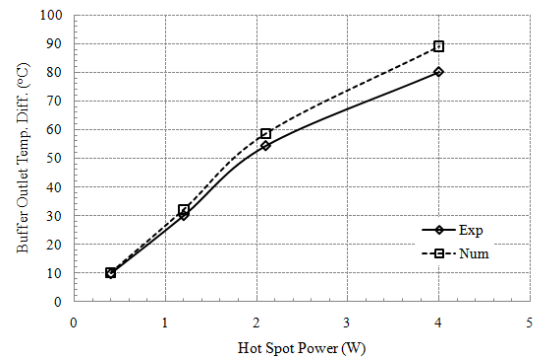


Fig. 4. Experimental and numerical cooling fluid outlet temperatures differences for different input powers at applied EOF voltage of 400 V

Nusselt number (Nu) variations for the microchannel are presented in Fig. 5. The bulk temperature was evaluated at various sections through the microchannel. Using the difference in the channel's wall temperature and the fluid bulk temperature and knowing the wall heat flux the heat transfer coefficient (h) was evaluated. Nusselt number was calculated using the (h) value, the channel hydraulic diameter, and the fluid thermal conductivity. Nusselt number was 5.39 at the channel entrance and decreased to a constant value of 4.56 for the rest of the channel as shown in Fig. 5.

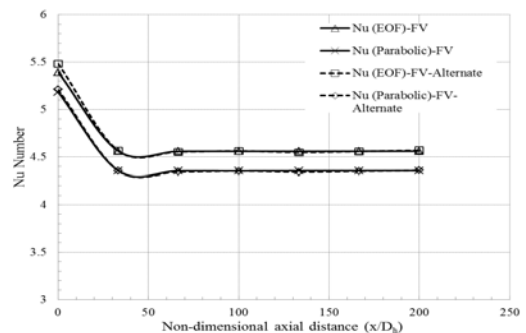


Fig. 5. Variation of Nu number along the non-dimensional length of the micro-channel for EOF and pressure-driven flows

For cross-checking the Nu values, an alternate finite volume (FV-Alternate) solver (ANSYS-Fluent, ANSYS, Inc., Canonsburg, PA) was used to calculate the numerical temperature distribution through the microchannel. To mimic the EOF, a microchannel with *slip walls* was constructed and uniform velocity was used as the inlet boundary condition instead of electric potential. Using a similar approach, Nu number was evaluated for the microchannel at the same flow and heat transfer conditions. Nusselt number was 5.48 at the channel entrance and decreased to a constant value of 4.56 for the rest of the channel as shown in Fig. 5. The Nu results of the FV and FV-Alternate solvers matched within 1%.

To compare Nu numbers for EOF and the conventional pressure-driven flow (parabolic velocity profile), numerical calculations of the temperature distribution were performed for the pressure-driven case. Both FV and FV-Alternate were used for the numerical calculations. For the FV solver, Nu number was 5.19 at the channel entrance and decreased to a constant value of 4.35 for the rest of the channel. For the FV-Alternate solver, Nu was 5.21 at the channel entrance and decreased to a constant value of 4.35 for the rest of the channel as shown in Fig. 5. These Nu numbers matched within 1%. It can be noticed that Nu number for the EOF flow was 5% higher than the case of the pressure driven flow.

Using the analytical method described in chapter 4 of Burmeister [10], analytical Nu numbers for EOF and pressure-driven flow were evaluated. The analytical Nu number for the EOF was 4.5 for the same geometry, flow, and heating conditions. The difference between the numerically and analytically calculated Nu numbers for the EOF was within 1.3%. The analytical Nu number for the pressure-driven flow was 4.07. This accounts to an enhancement of Nu number by 10.6% when the flow was changed from pressure-driven flow to EOF. Thus, comparing the FV methods and the analytical calculations, about 10% increase in Nu number is possible.

4 CONCLUSIONS

A micro-scale heat exchanger was designed and tested for different powers, and EOF voltages. Temperature differences of the cooling fluid between the microchannel outlet and inlet, as well as the substrate temperature were measured. The variation of Nusselt number was plotted along the non-dimensional channel length. Nusselt number for the EOF flow was 4.56 whereas it was 4.35 for the pressure-driven flow. Due to the plug-flow profile associated with the EOF Nusselt number of the EOF was about 10% higher than the pressure-driven flow (parabolic profile) flow.

It is evident that the joule heating increased with the increase in applied EOF voltage. This was observed when the EOF voltage was applied without the application of heat flux. This helped in determining the influence of joule heating with the increase in EOF voltage. For higher (e.g.,

400 V) EOF, the cooling fluid temperature got elevated appreciably due to joule heating which needs to be minimized. For a fixed heating power, the applied EOF voltage increases the electro-osmotic velocity leading to some increase in heat transfer while elevating the joule heating. Choosing an optimum range of EOF voltage helps reducing joule heating while increasing the overall heat transfer.

REFERENCES

1. Singhal, V., S.V. Garimella, and A. Raman, *Microscale pumping technologies for microchannel cooling systems*. Applied Mechanics Reviews, 2004. **57**(3): p. 191-221.
2. Jiang, L.N., et al., *Closed-loop electroosmotic microchannel cooling system for VLSI circuits*. Ieee Transactions on Components and Packaging Technologies, 2002. **25**(3): p. 347-355.
3. Laser, D.J., et al., *Silicon electroosmotic micropumps for integrated circuit thermal management*. Boston Transducers'03: Digest of Technical Papers, Vols 1 and 2, 2003: p. 151-154 1938.
4. Zhang, L., et al., *Measurements and modeling of two-phase flow in microchannels with nearly constant heat flux boundary conditions*. Journal of Microelectromechanical Systems, 2002. **11**(1): p. 12-19.
5. Jung, J.Y., H.S. Oh, and H.Y. Kwak, *Forced convective heat transfer of nanofluids in microchannels*. International Journal of Heat and Mass Transfer, 2009. **52**(1-2): p. 466-472.
6. Eng, P., P. Nithiarasu, and O. Guy, *An experimental study on an electro-osmotic flow-based silicon heat spreader*. Microfluidics and Nanofluidics: p. 1-9.
7. Dasgupta, S., et al., *Effects of applied electric field and microchannel wetted perimeter on electroosmotic velocity*. Microfluidics and Nanofluidics, 2008. **5**(2): p. 185-192.
8. Probstein, R., *Physicochemical hydrodynamics: an introduction*1994: Wiley-Interscience.
9. Comandur, K., et al., *Transport and reaction of nanoliter samples in a microfluidic reactor using electro-osmotic flow*. Journal of Micromechanics and Microengineering, 2010. **20**: p. 035017.
10. Burmeister, L., *Convective heat transfer*1993: Wiley-Interscience.